Thickness Mapping of the Occipital Bone on CT-data — a New Approach Applied on OH 9

Gerhard W. WEBER[1], Johann KIM[2], Arnold NEUMAIER[2], Cassian C. MAGORI[3], Charles B. SAANANE[3], Wolfgang RECHEIS[4], Horst SEIDLER[1]

(1. Institute for Anthropology, University of Vienna, Althanstr. 14, A-1090 Vienna. AUSTRIA; 2. Institute of Mathematics, University of Vienna, Strudlhofgasse 4, A-1090 Vienna, AUSTRIA; 3. Dept. of Anatomy & Histology, Muhimbili University College of Health Science, P.O. Box 65453, Dar-es Salaam, TANZANIA; 4. Dept. of Radiology II, University Hospital Innsbruck, Anichstr. 35, A-6020 Innsbruck, AUSTRIA)

Abstract

A new approach for the analysis of cranial bone thickness is introduced. The study focuses on the occipital bone of modern humans and of a 1.25 Myr-old *H. ergaster/erectus* specimen from Olduvai Gorge (OH 9). A semiautomatic algorithm detects a multitude of thicknesses from CT-data of the investigated bones. We find that every bone is characterized by its own distribution pattern of cranial thickness, which is then analyzed statistically. The results demonstrate that the thickness distribution of the occipital bone of OH 9 is within the normal range of the *H. sapiens* sample (which itself shows a remarkably high variance). This contributes to a further analysis of phyletic differences of hominid morphology by including distribution patterns of thickness combined with aspects of functional anatomy.

Key words: Occipital bone; Bone thickness; Hominid evolution; Virtual anthropology; Computed tomography

1 Introduction

Information about the thickness of cranial bones are not only of great medical interest, particularly for preoperative surgical planning [1], but can be as useful for investigations of fossil hominid material [2]. However, not much data is available for both these disciplines. Intra- and interspecific variation [3-4] is poorly known and mostly depends on measurements taken on a handful of landmarks or other not well defined points. These studies fall short of offering adequate information about the structural details of skulls, especially when considering specific endo- and exocranial qualities. Other authors [5-6] have undertaken efforts to develop thickness maps of the cranial vault but again with the restriction of a very limited number of measuring points.

We demonstrate a new approach, using CT-data of modern *Homo sapiens* skulls and of a skull of *Homo ergaster/erectus* from Tanzania, namely the 1.25 Myr-old OH 9. As the method is still under development we had to limit the formulation of the problem and so we are focusing on the occipital bone only. The points we use for the analysis are defined by the resolution of the CT-scan (0.4 mm). From every point on the surface of the bone we can measure the occipital thickness by using a new algorithm and the results can be given as a matrix as well as a topographical thickness map of the investigated bone. The method is part of our "**Virtual Anthropology**" project [7-9] concerned with the 3D-analysis of CT-data of recent and fossil hominids. The aim of the present study is to obtain a sufficient number of thickness measurements by a semiautomatic process to characterize the thickness distribution and to analyze the morphology variation of phyletic species.

2 Material

Our sample consists of 12 *H. sapiens* occipital bones (Table 1) and we tried to get as much variation as possible by including skulls from different populations (4 Europeans, 3 Africans, 3 Asians, 2 Australiens) of different sex (5 female, 7 males). Our first candidate of a fossil specimen to be compared was the occipital bone of the Tanzanian *H. ergaster/erectus* OH 9.

Table 1

Individuals in the study

Skull	Sex	Age	Origin	Notes
VA 1	Female	25	Europe	335
VA 2	Male	45	Europe	LE 54
VA 3	Male	25	Europe	NL 320
VA 4	Female	30	Europe	NL 371, HY
VA 13	Female	20	Australia	Aboriginal, C.80
VA 20	Male	40	Australia	Aboriginal, C.70
VA 23	Male	50	Africa	Bantu, S 66
VA 24	Female	20	Africa	Bantu, S 157
VA 25	Male	30	Africa	Bushman, S 60
VA 26	Male	35	Asia	Chinese, 2587
VA 27	Male	35	Asia	Chinese, 2576
VA 28	Female	30	Asia	Chinese, 2584
OH 9	-	-	Africa	Tanzania

3 Methods

3.1 Data

The occipital bones were isolated from the CT-data sets of the complete skulls with the software package ANALYZE AVW in such a way that the cut was roughly orthogonal to the surface along the sutures of the occipital bone. To avoid thickness artefacts of the occipital condyles, we decided to cut cross the foramen magnum approximately in the region of the condylarian canals. The data was then thresholded according to the HMH-standard method [10] and exported for the further mathematical procedure into a binary three dimensional matrix. Subsequent computations were performed in MATLAB 5.2.

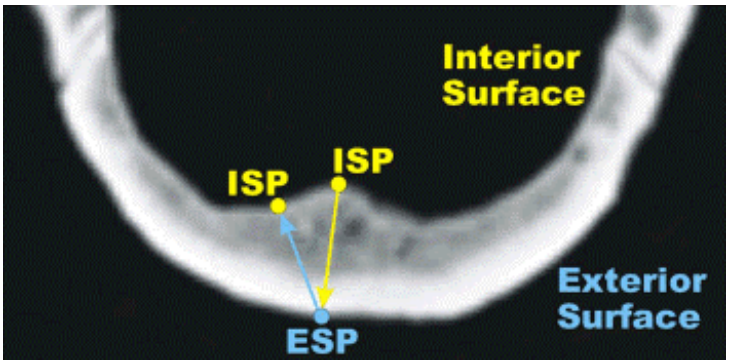

Figure 1 Computation of thickness on CT-scans of the occipital bone (here one slice); thickness measurements are not symmetric (blue: from outside to inside; yellow: from inside to outside)

3.2 Computation of the thickness

As many thicknesses as possible of the occipital bone were measured. For computation purposes mathematical definitions of biological categories included reductions. An occipital bone is a connected and bounded subset of the three dimensional space

$$\mathrm{OCC} \subseteq \nabla^3$$

The complementary set

$$\nabla^3 \setminus \mathrm{OCC}$$

is called outside. A surface point (SP) is an element of OCC and has a border to outside. An occipital bone has a surface S which is the set of all SP. Defining the bone by its interior and exterior surface is a first reduction because the cutting surface of the occipital bone is not considered. For the definition of the surfaces we need to introduce the observer's viewpoint which can be chosen as the center of gravity within the skull.

A surface point is called interior surface point (ISP) if the ray from the viewpoint to SP is a subset of the outside, i.e. no further point of OCC lies between the viewpoint and ISP. The interior surface (IS) is the set of all ISP. The exterior surface (ES) is the complementary set

$$\mathrm{S} \setminus \mathrm{IS}$$

i.e. an exterior surface point (ESP) is a SP which is not an ISP. The thickness d(ISP) at an ISP is the minimal distance from the ISP to ES.

$$d(ISP) = \min_{ESP \in ES} \Delta(ISP, ESP)$$

The measurement of thickness is not symmetric because, in general, the thickness measured from the interior surface is not the same as that measured from the exterior surface.

$$\Delta(ISP,ESP) \neq \Delta(ESP,ISP)$$

In practice, the data acquisition by CT-scanning includes a discretization of the set OCC from all points to a finite subset because OCC is approximated by voxels. A voxel is a volume element with x/y/z dimensions, comparable to pixels in 2D. Each voxel is represented by a triple of integers, so OCC is then a subset of $\wedge^3$, defining a discretized surface (DS). On an intact occipital bone of a *H. sapiens* approximately 100,000 points remain on the discretized interior surface (DIS). The computational costs for this number of points are still too high, so a reduction in the cardinality of DIS is necessary, ensuring no loss in geometric information.

The reduction of the DIS is obtained by a stepwise refinement of a starting triangulation.

1. A set of arbitrary points (lattice points) is initialized and the lattice is triangulated.
2. The edge is divided into two parts if the edge is longer than a given mesh size specified.
3. Step two is repeated until every edge is smaller than the mesh size.

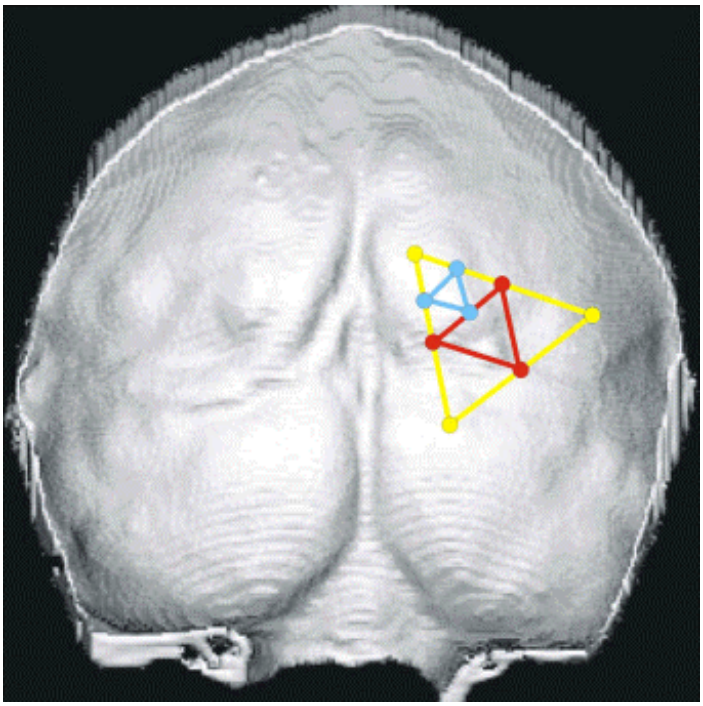

Figure 2 3D-reconstruction of the CT-data on the computer screen and scheme of triangulation procedure to further reduce the discretized interior surface (DIS)

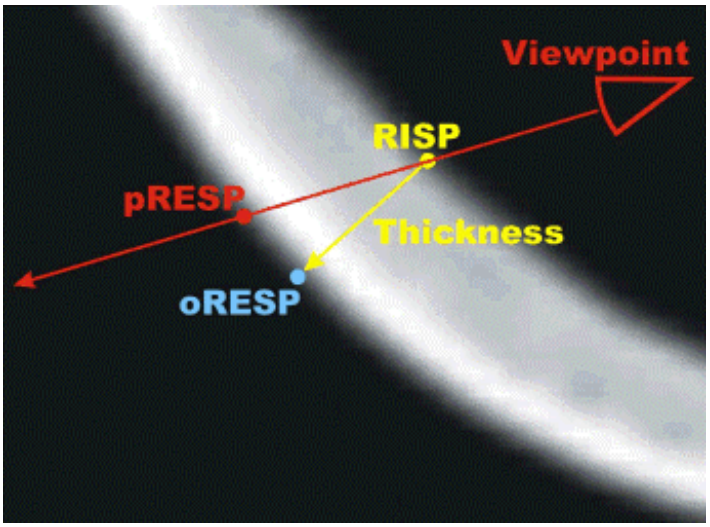

Figure 3 Thickness optimization procedure leads to the minimal distance between an interior surface point and its corresponding exterior surface point

The remaining points of DIS are called the reduced interior surface points (RISP). In order to compute the thickness over a RISP it is now necessary to find its corresponding reduced exterior surface point (RESP).

1. A first approximation of RESP (pRESP – provisional reduced exterior surface point) is found as the intersecting point of the discretized exterior surface (DES) and the line through the viewpoint and RISP.
2. pRESP is the starting point for a local optimization process which leads to the oRESP (optimal reduced exterior surface point). Starting with pRESP we find the adjacent neighbor DESP (not RESP) with the smallest distance to RISP. pRESP is overwritten by the neighbor DESP if the distance between RISP and DESP is smaller than the distance between RISP and pRESP.
3. Step two is repeated until no better DESP is found.

4 Results

In a first run, using a resolution of four voxels (thus we have a measuring point at least every 1.6 mm) the semiautomatic thickness measuring algorithm resulted in a number of measurements between 770 and 1,973 per occipital bone. Later, the number will be increased to 5,000 – 40,000 points.

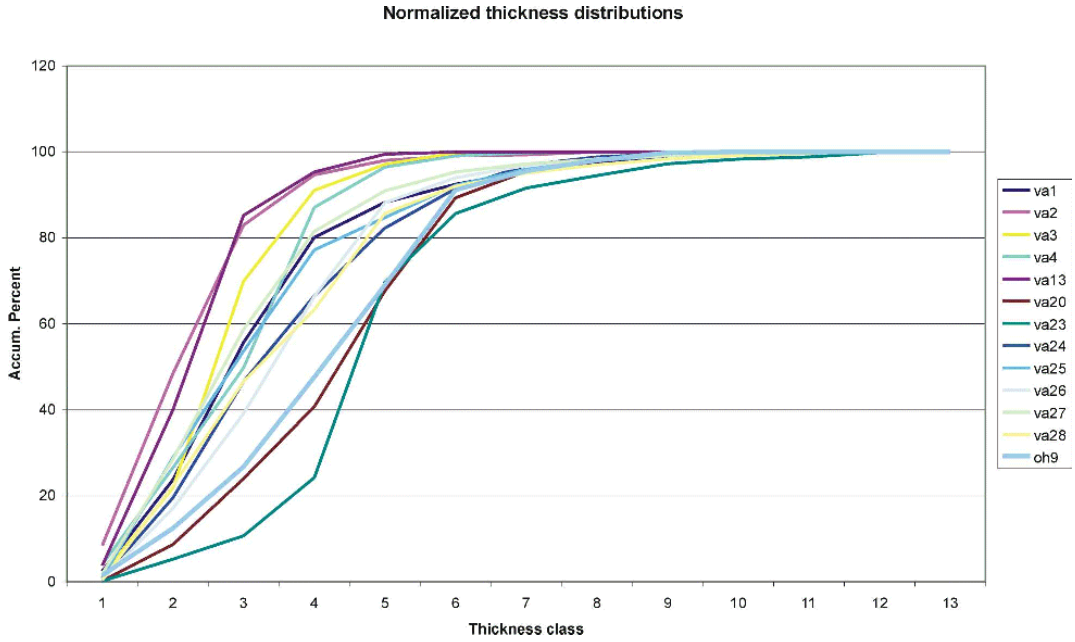

Figure 4 OH 9 lies within the range of variation of *Homo sapiens* (distribution of the normalized thicknesses)

For statistical analysis, the thickness distribution was approximated by a histogramm with 13 classes, ranging from 0 to 26 mm. To compensate for the different number of individual measurements on the bone, we normalized the data by computing the corresponding percentage for each class. The distributions of the normalized data are surprisingly heterogeneous among the moderns, but more surprising is the fact that OH 9 lies within this range. If parameters like the mean thickness, the median or the maximum of thickness are considered, OH 9 turns out to be on the upper end of the general distribution but has not one extreme value. VA 20, a male individual from Australia, and VA 23, a male individual from Africa, have higher means than OH 9. VA 1, VA 20, VA 23, VA 24, VA 25, VA 26, VA 27and VA 28 have higher maxima than does OH 9. Among these skulls are also female specimens (Table 2).

Table 2

Thickness of occipital bone

Skull	N	Mean	Std.dev.	Median	Min.	Max.
VA 1	1407	6.35	3.39	5.67	1.59	22.35
VA 2	770	4.34	2.14	4.13	1.49	15.94
VA 3	1513	5.37	1.87	5.13	1.59	12.62
VA 4	1412	5.73	2.27	6.01	1.49	14.14
VA 13	1160	4.53	1.73	4.47	1.59	11.46
VA 20	1350	8.52	3.18	8.70	1.82	20.75
VA 23	1311	**9.49**	3.36	**9.14**	1.82	**24.22**
VA 24	1383	6.97	3.25	6.19	1.67	22.30
VA 25	1286	6.38	3.43	5.78	1.49	19.46
VA 26	1298	7.01	3.00	6.92	1.89	20.39
VA 27	1440	6.01	3.08	5.58	1.67	20.62
VA 28	1101	7.03	**3.62**	6.64	1.89	23.78
OH 9	***1973***	***8.16***	***3.30***	***8.23***	***1.49***	***18.70***

The plot of the distributions of accumulated percentages (Fig. 4) makes it clear that the distribution of OH 9 is somewhat special compared with most *H. sapiens* skulls but two modern skulls show more deviation from these group than OH 9 does.

In a factor analysis (principal component) where all the relative frequencies in the 13 classes of thickness are variables, two major components which explain more than 88 % of the variance are extracted. Component one has high loads for the thickness classes 1, 2, 3, 5, 6 and 7 (0 – 6 mm, 8 – 14 mm), component two for 4, 5 and 6 (6 – 12 mm). The scatterplot of the two regression factor scores (Fig. 5) again shows that OH 9 lies well within the normal variation of our *H. sapiens* sample. Only VA 4 is remarkably distant to the cubic interpolation function plotted. A possible explanation for this is that VA 4 shows pathological changes on both the cranial base and the occipital condyles. The occipital of this female is relatively thin but has a very steep increase in thickness in the region of the internal occipital crest.

5 Discussion

5.1 Problems

As the data needs to be thresholded for accurate measurements to the average HMH values, small empty holes are created within the bone in the regions where the density of the spongious bone is very low (Figure 6). Our algorithm is therefore designed to cope with this problem and was robust enough.

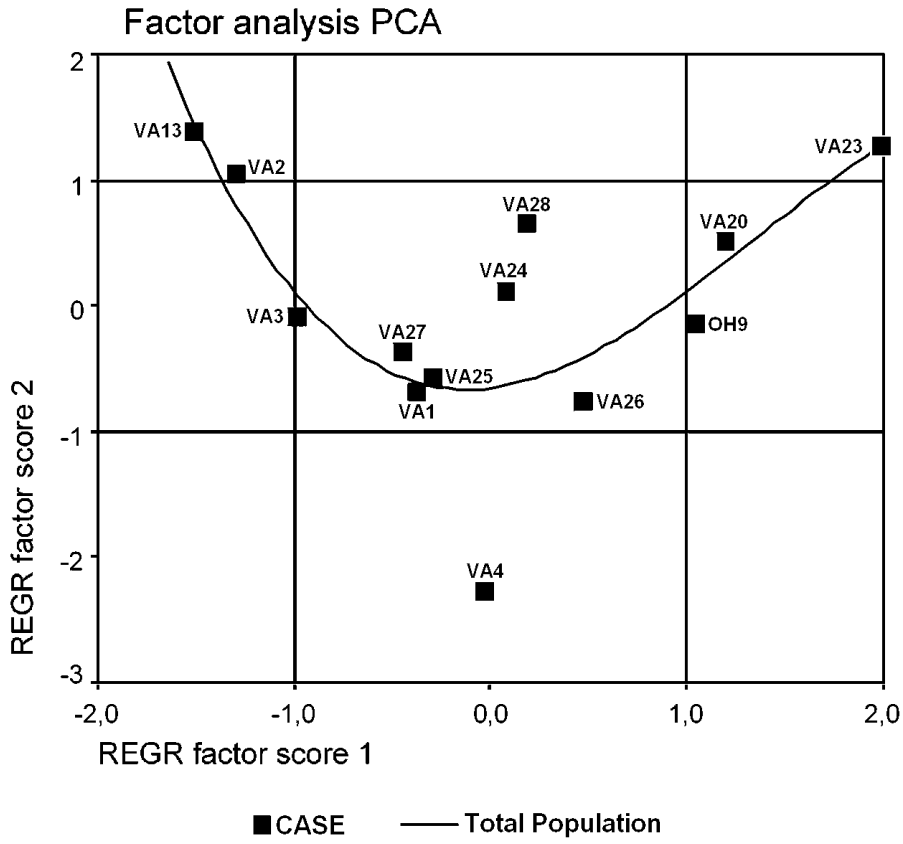

Figure 5 First two major components of the PCA explaining more than 88% of the variance. OH 9 fits well to the cubic interpolation function. The most distant individual VA 4 (H. sap.) is a pathological case

The position of the viewpoint to find the pRESP's can affect the results if the position is too far from the optimum. In a simulation with geometric objects we found a difference in mean thickness of around 8% for extreme positions. This problem only partly affects our results because the viewpoint was under our control and could always be placed in an acceptable location. Choosing different reasonable viewpoints and repeating the algorithm reduces the variability to an acceptably low value.

All lattice points of IS are within the actual margin, introducing a slight error, depending on how close to the margin the furthest lattice point is. Improvement by subdivision of lattice spacing solves this problem, but at the expense of increasing the number of lattice points in the set IS. The distribution analysis is sufficiently robust so that we feel confident in our results.

If the occipital bone is isolated and scanned, the CT-scan of the edges is highly serrated. As the triangulation process is restricted to a certain resolution, edge details are lost (Fig. 6, white points have no coordinates and are disregarded).

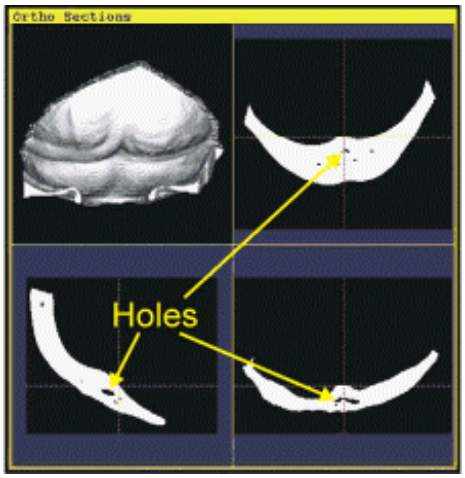

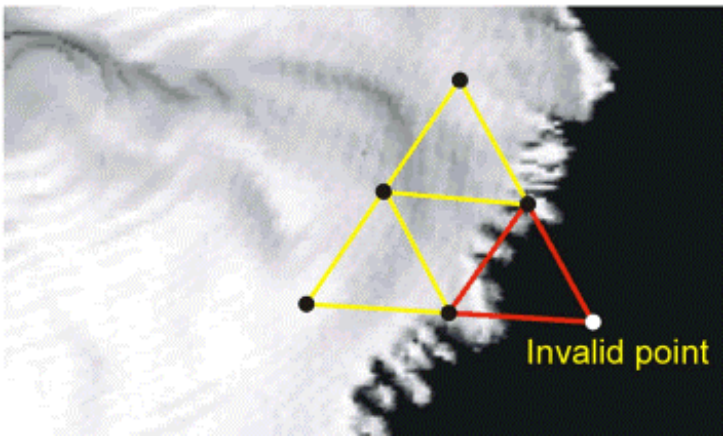

Figure 6 Small holes are created by the thresholding process in regions where the density of the spongious bone is low (above). The thickness algorithm is designed to cope with this problem. Some edge details are lost because the resolution of the triangulation process is limited (below). Using an appropriate meshsize, this effect hardly affects the distribution of thickness measurements

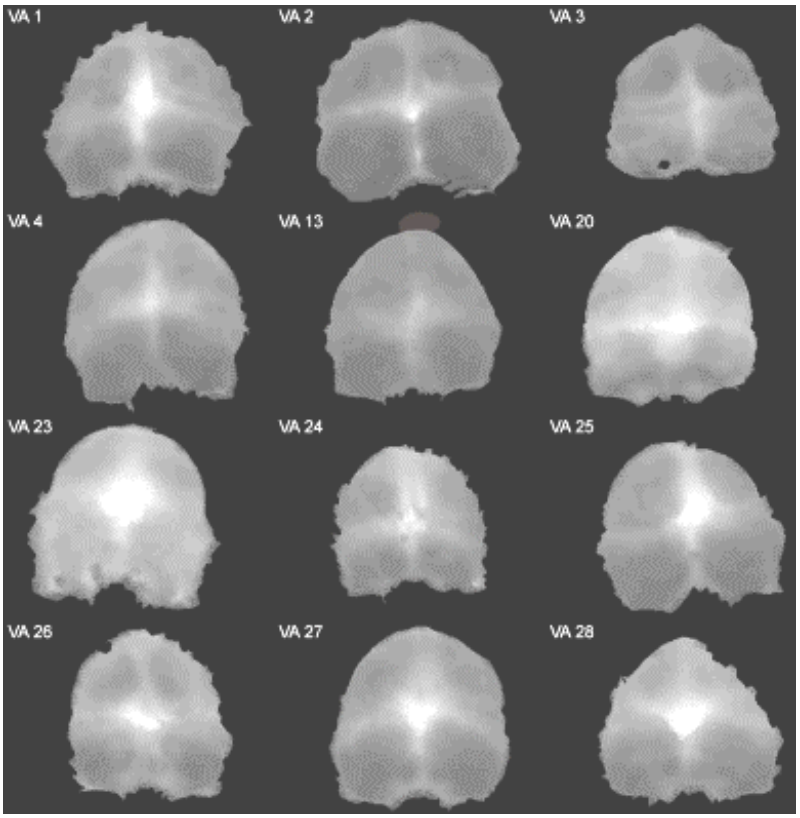

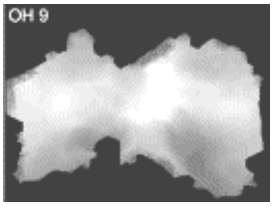

Figure 7 Topographical thickness plots of the 12 H. sap occipital bones and the one of OH 9; thin bone is dark gray, thick bone is white. Thickness distribution in defined regions can be analyzed

5.2 Conclusion

Being thought to be more massive than those of modern humans, the occipital bone of OH 9 demonstrates the relativity of this statement in a quantitative analysis with a sufficient number of thickness measurements. It is not enough to measure a few thicknesses to characterize an occipital bone adequately. It is more important to analyze the thickness distribution and to detect the peculiarities of this distribution in comparison with others. The topographical thickness plots (Fig. 7) of our measurements show some subtle structural differences. The occipital bone thickness of OH 9 seems to vary more regularly yet shows patterns similar to *H. sapiens* occipital bones if the occipital torus (thickened) or the cerebellar fossae (thinned) are included. Analysis of functional anatomy characterized by thickness distributions in defined regions should distinguish between different hominid morphologies. The high variance among *H. sapiens* occipital bone thickness and the similarity to a *H. ergaster/erectus* suggests that occipital bone thickness was not a feature under selection pressure within the last million years.

References:

[1] ELAHI MM, LESSARD ML, HAKIM S *et al*. Ultrasound in the assessment of cranial bone thickness [J]. J Craniofac. Surg, 1997, 8: 213-221.

[2] GAULD SC. Allometric patterns of cranial bone thickness in fossil hominids [J]. Am. J Phys Anthropol, 1996, 100: 411-426.

[3] LIEBERMAN DE. How and why humans grow thin skulls: experimental evidence for systemic cortical robusticity [J]. Am J Phys Anthropol, 1996, 101: 217-236.

[4] ZIPNICK RI, MEROLA AA, GORUP J *et al.* Occipital morphology. An anatomic guide to internal fixation [J]. Spine, 1996, 21: 1719-1724.

[5] ROSS AH, JANTZ RL & MCCORMICK WF. Cranial thickness in American females and males [J]. J Forensic Sci, 1998, 43(2): 267-272.

[6] HWANG K, KIM JH & BAIK SH. Thickness map of parietal bone in korean adults [J]. J Craniofac Surg, 1997, 8: 208-212.

[7] WEBER GW, RECHEIS W, SCHOLZE T *et al.* Virtual anthropology (VA): Methodological aspects of linear and volume measurements - First results [J]. Coll Antropol, 1998, 22: 575-583.

[8] CONROY GC, WEBER GW, SEIDLER H *et al.* Endocranial capacity in an early hominid cranium from Sterkfontein, South Africa [J]. Science, 1998, 280: 1730-1731.

[9] BOOKSTEIN F, SCHAEFER K, PROSSINGER H *et al.* Comparing frontal cranial profiles in archaic and modern *Homo* by morphometric analysis [J]. The Anatomical Record, 1999, 257: 217-224.

[10] Spoor CF, Zonneveld FW, Macho GA. Linear measurements of cortical bone and dental by computed tomography: applications and problems [J]. Am J Phys Anthropol, 1993, 91: 469-484.